Himanshu[1], Soumya Sarkar[2], Rupa Halder[2], Mita Biswas[2], Siddhartha Bandyopadhyay[2]*, Md. Farooq Wani[1]

[1] National Institute of Technology, Srinagar, J&K 190006, India
[2] CSIR-Central Glass and Ceramic Research Institute, Kolkata 700 032, India
Corresponding author. E-mail: sbando@cgcri.res.in

SPS PROCESSED TiB$_2$ REINFORCED Y-α-SiAlON COMPOSITES: HIGH TEMPERATURE TRIBOMECHANICAL PROPERTIES

Y-α-SiAlON and its composites containing 10 and 20 wt.% titanium diboride (TiB$_2$) were prepared using spark plasma sintering (SPS) at 1750°C for 10 minutes under 50 MPa. Although, the pure Y-α-SiAlON was > 97% dense, the increased TiB$_2$ content resulted in a slight reduction in the relative density of the composites (~2.6% max. at 20 wt.% TiB$_2$). In the presence of TiB$_2$ particulates, the impediment of grain boundary mass transport within the matrix grains might be responsible for such a reduced densification. The addition of TiB$_2$ resulted in a reduced Vickers hardness (HV$_1$), however, the indentation fracture toughness (K_{IC}) of Y-α-SiAlON increased upon an addition of TiB$_2$ up to 20 wt.%. While the HV_1 of the 20 wt.% TiB$_2$/Y-α-SiAlON composite was ~30% lower, the same composite offered around a 28% higher K_{IC} compared to pure Y-α-SiAlON. Unlubricated, reciprocating ball-on-disc experiments up to 500°C in ambient air indicated better wear resistance of the composites compared to pure Y-α-SiAlON up to a 90 N normal load.

Keywords: Y-α-SiAlON, TiB$_2$, composite, mechanical properties, tribology

INTRODUCTION

Owing to their attractive tribomechanical properties, e.g. high hardness, engineered toughness, resistance to chemical attack, better high temperature stability, improved metal cutting performance at a much higher speed and enhanced tool life compared to conventional carbide cutting inserts, SiAlON ceramics are gaining immense interest for the next generation of tribo-components for various high performance applications [1-6]. Although α-SiAlON ceramics possess a high hot hardness, the major limitation is their low toughness that restricts the wide-spread use of monolithic α-SiAlON as advanced tribo-elements [7]. To impart toughness and improved wear properties in various SiAlON phases, researchers have used different second phase particles, e.g., silicon carbide (SiC), titanium nitride (TiN), tungsten carbide (WC), molybdenum disilicide (MoSi$_2$), titanium carbonitride (Ti(C,N)), titanium diboride (TiB$_2$) etc. [1, 4, 8-13]. Bitterlich et al. [1] obtained the best wear resistance of a gas pressure sintered SiAlON composite reinforced with 10 vol.% SiC, whereas, due to some special effect, the MoSi$_2$/SiAlON composite offered adequate wear behaviour despite its poor hardness and toughness. Jones [4] reported the abrasive wear behavior of hot isostatically pressed TiB$_2$ reinforced SiAlON ceramics against an aqueous SiC (d_{50} = 5 μm) slurry. According to the report, the primary wear mechanism of the SiAlON composite was

the formation of a soft hydroxide or oxide layer through a tribochemical reaction between water and the matrix, followed by removal of the layer by the abrasive action of impinging SiC particles. In another work, Jones et al. [8] also highlighted the primary wear mechanism of the TiB$_2$/SiAlON composite in view of the formation and degradation of a tribofilm as well as the polishing of wear debris. According to the report by Abo-Naf et al. [9], the best wear properties were obtained for an Nd stabilized α/β-SiAlON composite because of the optimum presence of elongated grains to facilitate efficient crack deflection and bridging that reduced the material removal rate to the minimum. Zhao et al. [10] obtained the lowest wear rate of a 45 wt.% TiB$_2$/β-SiAlON composite primarily due to the presence of a refractory titanium compound in the matrix. Garrett et al. [11] achieved a more than 2 times higher toughness for an SPS processed 30 vol.% cBN/Y-α-SiAlON composite than the monolith (K_{IC} ≈ 3.7 MPa-m$^{0.5}$) principally due to crack deflection at the cBN/SiAlON interface that facilitated enhanced fracture energy dissipation. Biswas et al. [12] reported a more than 30% reduction in the specific wear rate (W_R) a 20 N normal load in the case of a spark plasma sintering (SPS) processed 15R-SiAlON polytype reinforced with 0.5 wt.% structurally stable multiwalled carbon nanotubes. Lee et al. [13] reported improved wear resistance of a hot isostatically pressed

15 vol.% SiC whisker reinforced α-SiAlON composite. In the present work an attempt was made to investigate the effect of 10 and 20 wt.% refractory TiB_2 particulate reinforcement in SPS processed yttria (Y_2O_3) doped α-SiAlON ceramics on their hardness, toughness and high temperature tribological performance.

EXPERIMENTAL PROCEDURE

Green batches of Y-α-SiAlON and its composites containing 10 and 20 wt.% TiB_2 particles were prepared using Si_3N_4, Y_2O_3, AlN, Al_2O_3 and TiB_2. The powder batches were prepared by mixing the base raw materials in appropriate proportions in an agate mortar pestle using acetone as the liquid medium for around 6 hours. The mixed powder was then dried in an air oven at 75^oC for volatile removal and collection. The samples were sintered using SPS (HP-D-25, FCT Systeme GmbH, Germany) at 1750^oC with a 10 minute dwell time under 50 MPa uniaxial pressure in argon atmosphere to obtain disc shaped samples (ϕ = 30 mm x t = = 6 mm). Both the heating and cooling rates were kept constant at 100^oC/min. The sintered pure SiAlON, 10 and 20 wt.% TiB_2 reinforced composites are designated as S0T, S10T and S20T, respectively, in rest of this report. The *Archimedes* water immersion technique was used to measure the sintered densities and porosities of the samples. The Vickers hardness (*HV*) and indentation toughness (K_{IC}) were measured under 9.8 N. The toughness values were calculated using well-known equations proposed by Niihara et al. [14, 15]. Unlubricated, high temperature tribological tests of the samples against a dense Si_3N_4 ball were conducted using a reciprocating ball-on-disk configuration (TR-20-M-57, DUCOM Instruments, Asia). For comparative study, all the wear tests were performed under identical conditions of 8.33 Hz, 2 mm stroke length. The variables were sliding distance (14, 28, 42, 56 and 70 m), normal load (20, 50 and 90 N) and test temperature (100, 200, 300, 400 and 500^oC). The primary output parameters were the coefficient of friction (COF) and W_R.

RESULTS AND DISCUSSION

Densification

Table 1 shows the density data of the sintered samples. The theoretical density values of the samples were calculated using the *rule of mixtures* taking the density of α-SiAlON and TiB_2 as 3.28 and 4.52 g/cc, respectively [16-18]. The open porosities of all the samples were calculated to be < 1% in all cases and hence were treated as negligible in this study. It can be seen from Table 1 that an increased TiB_2 content resulted in a slight but gradual decrease in the relative density (RD) of the composites. The reduction in the RD of the composites compared to the monolith is the resultant of two opposite phenomena. Firstly, it might have arisen

due to grain boundary mass transport inhibition in the presence of dispersed TiB_2 particulates. The second phenomenon, on the contrary, was the enhancement of sintering that counter balances the above reduction. The extremely low electrical resistivity ($\sim 10^{-7}$ Ω-cm) and high thermal conductivity (> 60 W/m-K) of the dispersed TiB_2 particulates [18] in the electrically insulating SiAlON matrix presumably established additional current conduction paths during the SPS cycle to promote enhanced Joule heating of the surrounding matrix and might have compensated as far as possible the resistance towards achieving adequate densification by the refractory second phase particulates. Hence, such a reduction in the RD values of the composites, i.e. $\sim 2.6\%$ (max.) at 20 wt.% TiB_2 loading in the SiAlON matrix, might be justified. The density values of α-SiAlON and the TiB_2/α-SiAlON composites matched well with the available literature data on similar materials processed via different routes [1, 4, 8, 10, 17]. Typical light micrographs of the studied samples are shown in Figure 1a-c. The distribution of second phase particulates, i.e., TiB_2 in the α−SiAlON matrix has been indicated with arrows (Fig. 1b-c).
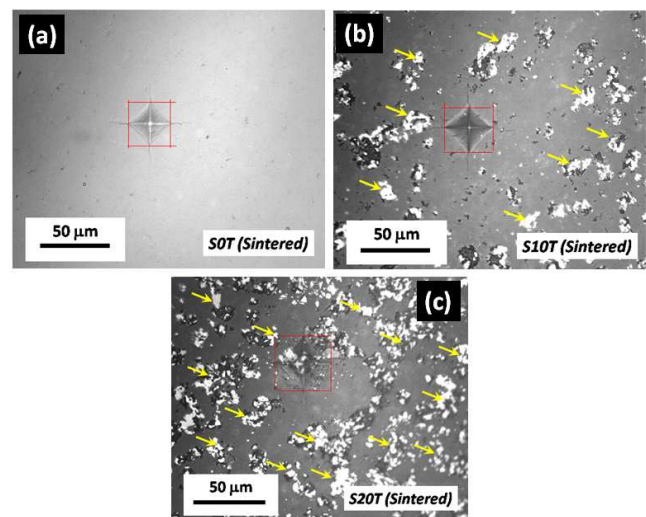

Fig. 1. Microstructures showing distribution of secondary phase and indentation mark of: a) pure Y-α-SiAlON; b) 10 wt.% TiB_2/Y-α-SiAlON composite and c) 20 wt.% TiB_2/Y-α-SiAlON composite

Table 1. Densification data of studied samples

Sample id	Theoretical density [g/cc]	Relative density [%]	HV_1 [GPa]	K_{IC} [MPa-m$^{0.5}$]
S0T	3.28	99.70	19.05 ±0.65	3.87 ±0.22
S10T	3.37	98.74	16.09 ±0.87	4.66 ±0.28
S20T	3.47	97.11	12.92 ±0.79	4.94 ±0.39

Vickers hardness and toughness

Despite the high hardness of monolithic TiB_2 [18], the presence of dispersed TiB_2 particulates in the SiAlON matrix resulted in a significant decrease in the

HV$_1$ data (Table 1). At 10 and 20 wt.% TiB$_2$ contents, around 16 and 32% reductions in the hardness values were obtained, respectively, compared to pure α-SiAlON (Table 1). A reduction in hardness was also obtained by others for theTiB$_2$/SiAlON composite due to extended grain growth of the TiB$_2$ particulates [17]. However, the formation of a weak interface between the constituent phases of the composites could also be a possible reason behind such a hardness reduction where easy deformation of both the phases under the applied load resulted in such reduced HV values. Contrary to that, the toughness values of the composites were found to be higher at an increased TiB$_2$ concentration in the matrix phase (Table 1). The 20 wt.% TiB$_2$/α-SiAlON composite offered around a 28% higher K_{IC} compared to the monolith (Table 1). Enhanced fracture energy dissipation through crack deflection at the weak TiB$_2$/α-SiAlON interface possibly resulted in toughness improvement of the composites. Analogous to the present result, Jones et al. [4] also obtained indentation toughness values in the range of 4.5÷5.7 MPa-m$^{0.5}$ for hot isostatically pressed 40 vol.% TiB$_2$/SiAlON composites when processed under different temperatures and pressures. Typical indentation marks are shown in Figure 1a-c.

Reciprocating wear behaviour

Reciprocating sliding distance test

The effect of increasing the sliding distance on the COF and W_R of all the three samples against the Si$_3$N$_4$ ball at 500°C and under a 50 N normal load was assessed by increasing the sliding distance up to 70 m with a periodic interval of 14 m. From Figure 2a it can be seen that a periodic increase in the sliding distance resulted in an increased COF for all the samples within the span of 0.34−0.52.

This was most likely caused by interaction of the worn out Si$_3$N$_4$ ball with the tribolayer and/or wear debris retained within the wear track of the preceding runs instead of direct interaction of a fresh ball with a polished surface. The COF values obtained in the present study during the sliding distance test for the TiB$_2$/α-SiAlON composites matched well with earlier literature data on different SiAlON matrix composites and related materials [9, 10, 13, 19]. On the contrary, irrespective of the sample composition, an increasing sliding distance resulted in a reduced wear rate (Fig. 2b).

In the case of pure α-SiAlON, the formation of an amorphous Si(OH)$_4$ layer through tribochemical reactions at 500°C in ambient air under 50 N most likely resulted in the observed reduced wear rate [9]. For the composites, besides improved toughness in relation to the monolith which restricted the material removal rate, simultaneous oxidation of the TiB$_2$ particulates along with the matrix phase might have also produced TiO$_2$(s) and B$_2$O$_3$(l) that contributed to tribofilm formation and resulted in a reduced wear rate (Fig. 2b) [20, 21].

The W_R of the 10 wt.% TiB$_2$/α-SiAlON composite after 70 m of sliding was found to be around 0.5 times lower than that obtained after 14 m of sliding under 50 N at 500°C. Similarly, the W_R of the 20 wt.% TiB$_2$/α-SiAlON composite after 70 m sliding was found to be nearly 0.34 times lower than that obtained after 14 m of sliding (Fig. 2b).
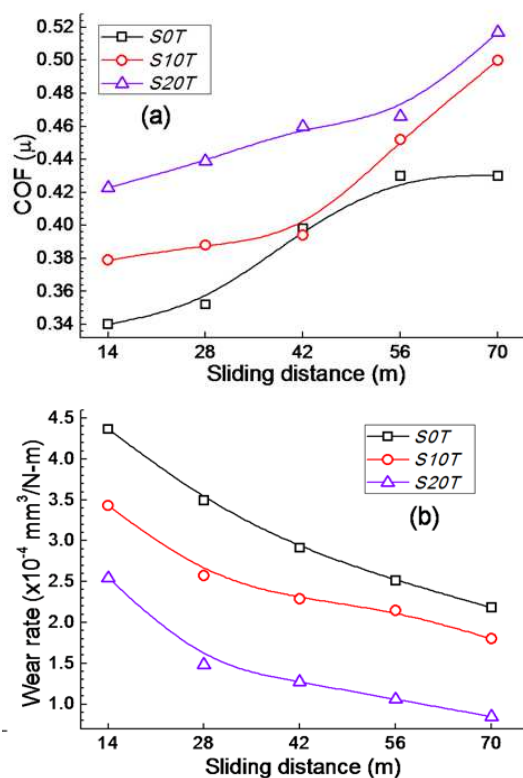

Fig. 2. COF vs. sliding distance and (a) W_R vs. sliding distance plots of samples (b)

Reciprocating load test

Under this test condition, the applied normal load varied from 20 to 90 N while maintaining the test temperature and sliding distance fixed at 500°C and 14 m, respectively. It can be seen from Figure 3a that irrespective of the sample composition, the COF values decreased with an increasing normal load. The most prominent decrease in COF (around 30%) was observed for the 20 wt.% TiB$_2$/α-SiAlON composite. This was possibly caused by the polishing action of wear debris as described by Jones et al. [8]. However, the W_R values increased steadily with an increase in applied normal load (Fig. 3b). This happened because at the increased load, the penetration depth of the counterbody into the sample discs was higher, resulting in a higher specific wear rate (Table 1). On the contrary, irrespective of the applied test load, reduced W_R values of the composites compared to the monolith indicated the positive effect of enhanced toughness and the formation of a mixed tribofilm that presumably counterbalanced the adverse effect of reduced hardness, especially, for the composites (Fig. 3b). The 10 wt.% TiB$_2$/α-SiAlON composite offered around 0.84÷0.74 times lower

W_R values compared to the monolith (W_R at 20N $\approx$ $\approx$ 3.1 x 10^{-4} mm^3/N-m; W_R at 50 N $\approx$ 4.4 x 10^{-4} mm^3/N-m; W_R at 90 N $\approx$ 5.2 x 10^{-4} mm^3/N-m). On the other hand, the 20 wt.% TiB$_2$/α-SiAlON composite offered nearly 0.3÷0.6 times lower W_R values compared to the pure α-SiAlON within a 20÷90 N normal load (Fig. 3b).
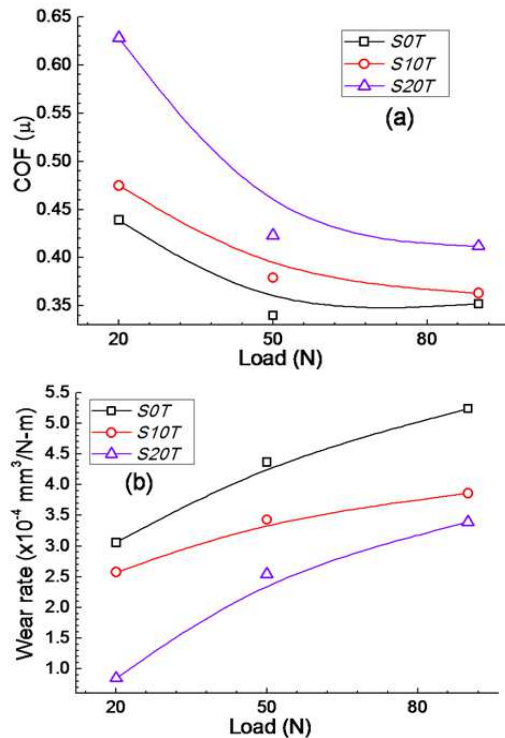

Fig. 3. *COF* vs. normal load and (a) W_R vs. normal load plots of samples (b)

Reciprocating temperature test

Except for the 20 wt.% TiB$_2$/α-SiAlON composite, an increase in test temperature resulted in a continuous decrease in *COF* values (Fig. 4a). The maximum drop in *COF* was noticed for the monolith (from 0.53 at 100°C to 0.34 at 500°C) followed by the 10 wt.% TiB$_2$/α-SiAlON composite (from 0.47 at 100°C to 0.38 at 500°C) (Fig. 4a). On the contrary, the COF of the 20 wt.% TiB$_2$/α-SiAlON composite remained almost constant at around 0.43 at all the test temperatures. The formation of an amorphous Si(OH)$_4$ tribofilm for pure α-SiAlON and mixed tribolayer for the 10 wt.% TiB$_2$/SiAlON composite presumably contributed to reducing the contact severity at the ball/disc interface at increased test temperatures and eventually, resulted in a reduced COF. On the other hand, despite the mixed tribofilm formation at increased test temperatures, the improved toughness possibly resisted progressive material removal from the disc sample, creating a more harsh condition at the ball/disc interface that might have resulted in an almost constant COF for the 20 wt.% TiB$_2$/α-SiAlON composite (Fig. 4a), despite its lower hardness that was supposed to permit greater penetration of the counterbody. Increasing the test temperature always resulted in higher wear rates for the studied

samples (Fig. 4b). The expected formation of a tribofilm through tribochemical reaction at increased test temperatures followed by its detachment from the wear track to create a fresh surface for additional wear possibly resulted in the such observed enhanced wear rate at higher test temperatures. However, the improved toughness of the composites offered ~0.7÷0.8 times lower W_R values for the 10 wt.% TiB$_2$/α-SiAlON composite and ~0.2÷0.6 times lower wear rates for the 20 wt.% TiB$_2$/α-SiAlON composite compared to the pure α-SiAlON at increasing test temperatures. At $\leq$ 200°C, the higher toughness of the 20 wt.% TiB$_2$/α-SiAlON composite compared to the monolith effectively hindered material removal from the composite sample that resulted in an almost 0.2÷0.3 times lower W_R for the 20 wt.% TiB$_2$/α-SiAlON composite than those obtained for pure α-SiAlON (Fig. 4b). Beyond 200°C, progressively higher thermomechanical stresses at the interface region presumably helped to form an increasing amount of Si(OH)$_4$ and TiO$_2$(s) and B$_2$O$_3$ (l) to enhance the wear rate of the composite through subsequent detachment of the formed tribolayer. As a result, the W_R values of the same composite within the 300÷500°C test temperature range were found to be almost 0.5÷0.6 times lower compared to those obtained for the monolith (Fig. 4b).
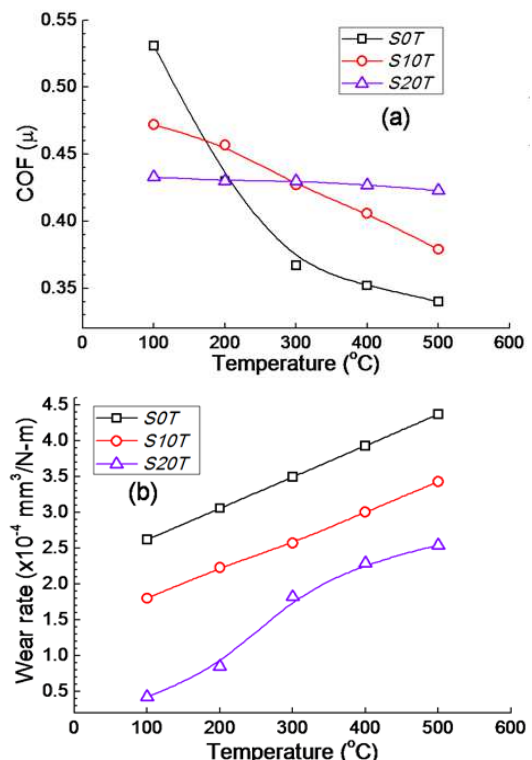

Fig. 4. *COF* vs. test temperature (a) and W_R vs. test temperature plots of samples (b)

CONCLUSIONS

Dense (> 97%) Y-α-SiAlON and its composites containing 10 and 20 wt.% TiB$_2$ particulates were success-

fully prepared using SPS at 1750°C under 50 MPa for 10 minutes. The observed 16÷32% reduction in hardness values of the composites compared to the pure SiAlON might have resulted from the weak interface between the matrix and reinforcement. In contrast, enhanced fracture energy dissipation through crack deflection at the weak interface regions could have resulted in a higher toughness of the composites. The 20 wt.% TiB$_2$/α-SiAlON composite offered around a 28% higher K_{IC} compared to the monolith ($K_{IC} \approx$ ≈ 3.9 MPa-m$^{0.5}$). Owing to the improved toughness of the composites that restricted material loss through intergranular microfracture and the expected formation of a mixed hydroxide/oxide tribofilm, the composites offered better wear resistance compared to the pure α-SiAlON. At increased test loads from 20÷90 N, the 20 wt.% TiB$_2$/α-SiAlON composite offered around 0.3÷0.6 times lower W_R values than those obtained for the pure α-SiAlON (W_R at 20N $\approx$ 3.1 x 10^{-4} mm^3/N-m; W_R at 50 N $\approx$ 4.4 x 10^{-4} mm^3/N-m; W_R at 90 N $\approx$ ≈ 5.2 x 10^{-4} mm^3/N-m). Similarly, at lower test temperatures i.e., ≤ 200°C, the 20 wt.% TiB$_2$/α-SiAlON composite offered an 0.2÷0.3 times lower wear rate than those obtained for pure α-SiAlON (W_R at 100°C $\approx$ ≈ 2.6 x 10^{-4} mm^3/N-m; W_R at 200°C $\approx$ 3.1 x 10^{-4} mm^3/N-m). In contrat, the likely formation of increased amounts of Si(OH)$_4$, TiO$_2(s)$ and B$_2$O$_3$ (l) at higher test temperatures resulted in an enhanced wear rate of the composite through subsequent spallation of the formed tribolayer. As a consequence, the 20 wt.% TiB$_2$/α-SiAlON composite offered W_R values which were found to be 0.5÷0.6 times lower compared to the monolith within the 300÷500°C range.

Acknowledgements

REFERENCES

[1] Bitterlich B., Bitsch S., Friederich K., SiAlON based ceramic cutting tools, J. Eur. Ceram. Soc. 2008, 28, 989-994.

[2] Cao G.Z., Metselaar R., α'-SiAlON ceramics: A review, Chem. Mater. 1991, 3, 242-252.

[3] Hampshire S.H., Park K., Thompson D.P. et al., α-SiAlON ceramics, Nature 1978, 274, 880-882.

[4] Jones A.H., Micro-scale abrasive wear of silicon nitride, sialon-TiB$_2$ composites and D$_2$ tool steel using a multiple load method, Wear 2005, 258, 942-952.

[5] Bandyopadhyay S., Hoffman M.J., Petzoe G., Densification behavior and properties of Y$_2$O$_3$ containing α-SiAlON based composites, J. Am. Ceram. Soc. 1996, 79, 1537-1545.

[6] Bandyopadhyay S., The in situ formation of SiAlON composite phases, J. Eur. Ceram. Soc. 1997, 17, 929-934.

[7] Kato K., Adachi K., Wear of advanced ceramics, Wear, 2002, 253, 1097-1104.

[8] Jones A.H., Dobedoe R.S., Lewis M.H. et al., SiAlON/TiB$_2$ ceramic composites: synthesis, properties and tribology, Brit. Ceram. Trans. 1999, 98, 274-281.

[9] Abo-Naf S.M., Dulias U., Schneider J. et al., Mechanical and tribological properties of Nd- and Yb-SiAlON composites sintered by hot isostatic pressing, J. Mater. Proc. Technol. 2007, 183, 264-272.

[10] Zhao Y.S., Yang Y., Li J.T., et al., Combustion synthesis and tribological properties of SiAlON based ceramic composites, Int. J. Self. Propag. High Temp. Synth. 2010, 19, 172-177.

[11] Garrett J.C., Sigalas I., Herrmann M., et al., cBN reinforced Y-α-SiAlON composites, J. Eur. Ceram. Soc. 2013, 33, 2191-2198.

[12] Biswas M., Sarkar S., Bandyopadhyay S., Improvements in mechanical properties of SPS processed 15R-SiAlON polytype through structurally survived MWCNT reinforcement, Mater. Chem. Phys. 2019, 222, 75-80.

[13] Lee B.-H., Kim I.-S., Lee K.-H., Mechanical and tribological properties of α-SiAlON/SiC whisker composites, J. Kor. Ceram. Soc. 1993, 30, 785-790.

[14] Niihara K., Morena R., Hasselman D.P.H., Evaluation of K$_{IC}$ of brittle solids by the indentation method with low crack-to-indent ratios, J. Mater. Sci. Lett., 1982, 1, 13-16.

[15] Niihara K., A fracture mechanics analysis of indentation-induced Palmqvist crack in ceramics, J. Mater. Sci. Lett. 1983, 2, 221-223.

[16] Shan Y., Wang G., Liu G. et al., Hot-pressing of translucent Y-α-SiAlON ceramics using ultrafine mixed powders prepared by planetary ball mill, Ceram. Int. 2014, 40, 11743--11749.

[17] Vleugels J., Jiang D.T., Van der Biest O., Development and characterisation of SiAlON composites with TiB$_2$, TiN, TiC and TiCN, J. Mater. Sci. 2004, 39, 3375-3381.

[18] Jones A.H., Dobedoe R.S., Lewis M.H. et al., Mechanical properties and tribology Si$_3$N$_4$-TiB$_2$ ceramic composites produced by hot pressing and hot isostatic pressing, J. Eur. Ceram. Soc. 2001, 21, 969-980.

[19] Xie Z.H., Hoffman M., Moon R.J. et al., Sliding wear of Ca–α–SiAlON ceramics at 600°C, Wear 2006, 206, 1356--1360.

[20] Yang Z.-L., Ouyang J.-H., Liu Z.-G., Isothermal oxidation behavior of reactive hot-pressed TiN-TiB$_2$ ceramics at elevated temperatures, Mater. Des. 2011, 32, 29-35.

[21] Shahbahrami B., Bastami H., Shahbahrami N., Studies on oxidation behaviour of TiB$_2$ Powder, Mater. Res. Innovations 2010, 14, 107-109.